

# Prestimulation phase predicts the TMS-evoked response

Bornali Kundu, Jeffrey S. Johnson and Bradley R. Postle

*J Neurophysiol* 112:1885-1893, 2014. First published 9 July 2014; doi:10.1152/jn.00390.2013

## You might find this additional info useful...

---

This article cites 37 articles, 20 of which can be accessed free at:

</content/112/8/1885.full.html#ref-list-1>

Updated information and services including high resolution figures, can be found at:

</content/112/8/1885.full.html>

Additional material and information about *Journal of Neurophysiology* can be found at:

<http://www.the-aps.org/publications/jn>

---

This information is current as of January 15, 2015.

## Prestimulation phase predicts the TMS-evoked response

Bornali Kundu,<sup>1</sup> Jeffrey S. Johnson,<sup>2</sup> and Bradley R. Postle<sup>2,3</sup>

<sup>1</sup>Medical Scientist Training Program and the Neuroscience Training Program, University of Wisconsin-Madison, Madison, Wisconsin; <sup>2</sup>Department of Psychiatry, University of Wisconsin-Madison, Madison, Wisconsin; and <sup>3</sup>Department of Psychology, University of Wisconsin-Madison, Madison, Wisconsin

Submitted 29 May 2013; accepted in final form 8 July 2014

**Kundu B, Johnson JS, Postle BR.** Prestimulation phase predicts the TMS-evoked response. *J Neurophysiol* 112: 1885–1893, 2014. First published July 9, 2014; doi:10.1152/jn.00390.2013.—Prestimulation oscillatory phase and power in particular frequency bands predict perception of at-threshold visual stimuli and of transcranial magnetic stimulation (TMS)-induced phosphenes. These effects may be due to changes in cortical excitability, such that certain ranges of power and/or phase values result in a state in which a particular brain area is more receptive to input, thereby biasing behavior. However, the effects of trial-by-trial fluctuations in phase and power of ongoing oscillations on the brain's electrical response to TMS itself have thus far not been addressed. The present study adopts a combined TMS and electroencephalography (EEG) approach to determine whether the TMS-evoked response is sensitive to momentary fluctuations in prestimulation phase and/or power in different frequency bands. Specifically, TMS was applied to superior parietal lobule while subjects performed a short-term memory task. Results showed that the prestimulation phase, particularly within the beta (15–25 Hz) band, predicted pulse-by-pulse variations in the global mean field amplitude. No such relationship was observed between prestimulation power and the global mean field amplitude. Furthermore, TMS-evoked power in the beta band fluctuated with prestimulation phase in the beta band in a manner that differed from spontaneous brain activity. These effects were observed in areas at and distal to the stimulation site. Together, these results confirm the idea that fluctuating phase of ongoing neuronal oscillations create “windows of excitability” in the brain, and they give insight into how TMS interacts with ongoing brain activity on a pulse-by-pulse basis.

transcranial magnetic stimulation; electroencephalography; phase; power; excitability

SPONTANEOUS FLUCTUATIONS in ongoing brain activity have been shown to exist within well-defined networks and have been linked to behavior (Schroeder and Lakatos 2009; Palva and Palva 2011). For example, the prestimulus phase and power of oscillations in the alpha-frequency band (ranging from 8 to 14 Hz) recorded at occipital channels have been shown to predict the perception of at-threshold visual stimuli (Van Dijk et al. 2008; Mathewson et al. 2009; Wyart and Tallon-Baudry 2009). These studies lend credence to the proposal that the brain's self-generated oscillations create a temporal context for the brain's network connectivity to behave under and respond to, which then translates into behavioral output (Buszák and Draguhn 2004). Generally, across studies, low prestimulus power has been found to predict signal detection, and high power predicts failure-to-detect (cf. Babiloni et al. 2006). Additionally, low prestimulus alpha-band power (roughly de-

finer as 8–12 Hz) predicts higher amplitude of the blood-oxygen level-dependent response evoked by visual stimulation (Scheeringa et al. 2009), as measured by functional magnetic resonance imaging. The instantaneous phase, windowed to encompass the time interval immediately before stimulus onset, also predicts the probability of stimulus detection (Busch et al. 2011; Busch and VanRullen 2010). In the case of alpha-band oscillations, the neural bases of these effects have been proposed to reflect the “pulsed-inhibition” of ongoing neural activity (Mathewson et al. 2009), a corollary of the idea that ensembles that oscillate in the alpha-frequency range can no longer effectively process information (Jensen and Mazaheri 2010). In another line of research, Lange et al. (2013) used visual illusions to test whether prestimulus alpha-band power related to veridical perception. They found that low prestimulus alpha-band power was a better indicator of whether a subject reported a stimulus than of veridical perception per se. They, along with others, suggest that prestimulus alpha-band power might determine instantaneous cortical excitability and that this state of excitability is subject to change moment-by-moment. In this context, excitability implies a momentary brain state in which, for example, the visual cortex is more receptive to input from another brain area.

Another line of work, in the nonhuman primate, has implicated a role for oscillations in the beta band (roughly 15–25 Hz) in “clocking” behavioral functions such as shifts of attention and the generation of eye movements (Buschman and Miller 2009). The beta band may also be an important frequency band for the implementation of top-down control via long-range phase synchronization (Engel and Fries 2010).

Transcranial magnetic stimulation (TMS) can be used to induce weak electrical currents in targeted tissues, thereby altering ongoing neural activity (Walsh and Pascual-Leone 2005). Incorporating TMS with electroencephalography (EEG) has made it possible to directly observe the effects of TMS on this activity. TMS of visual cortex at particular intensities can induce the perception of phosphenes, a phenomenon characterized by the subjective experience of brief light flashes in the absence of light entering the eye. The probability of TMS-induced phosphene perception has been used to operationalize cortical excitability in humans, and the probability of a subject reporting TMS-induced phosphenes is correlated with trial-by-trial fluctuations in the prestimulation power (Romei et al. 2008) and phase (Dugué et al. 2011) of alpha-band oscillations. These studies suggest that TMS may interact with underlying brain oscillations such that the phase and power of these oscillations predict the effects of TMS on subsequent behavior. Romei et al. (2008) suggest that signal detection may depend on fluctuations in cortical excitability, such that low prestimu-

Address for reprint requests and other correspondence: B. Kundu, Dept. of Psychiatry, Univ. of Wisconsin-Madison, 6001 Research Park Blvd., Madison, WI 53719 (e-mail: bkundu@wisc.edu).

lation alpha-band power is thought to correspond to a state in which the cortex is more receptive to input, in this case, by TMS-induced current.

A limitation of task-related visual perception and of phosphene perception, however, is that both are indirect measures of cortical excitability and connectivity, in that they, presumably, reflect the result of several electrophysiological steps after stimulation. What does “increased excitability” look like at the network level in the whole brain? One way to investigate this is to assess whether the TMS-evoked response (TMS-ER) itself is influenced by the prestimulation phase and/or power. Unfortunately, in the case of the phosphene perception paradigm, the visual-evoked potential produced by visual cortex as a result of perceiving the phosphene will necessarily confound the measurement of the TMS-ER itself. Thus, in the present study, we investigated whether trial-by-trial variations in prestimulation phase and/or power influenced properties of the TMS-ER to single pulses delivered to the superior parietal lobule (SPL) during the delay period of a spatial short-term memory (STM) task. The data were drawn from a previously published study that showed that the TMS-ER differed depending on whether TMS was applied during the performance of the STM task vs. during a perceptually identical period of fixation (Johnson et al. 2012). Crucially, the site of stimulation ensured that there was no perceptual evoked response from TMS in this task context.

Results revealed that spontaneous fluctuations in prestimulation phase within the beta-frequency band had a systematic effect on the amplitude and spectral properties of the TMS-ER. No such effects were found for prestimulation power. These findings provide direct support for the idea that moment-by-moment changes in underlying, spontaneous oscillations, as indexed by changes in prestimulation phase, perhaps more so than power, may drive trial-by-trial variations in behaviors, such as visual perception, through changes in cortical excitability and/or connectivity.

## METHODS

### Subjects

Sixteen subjects recruited from the University of Wisconsin-Madison community participated in the study [8 males, mean age = 21.9 (SD = 2.9)], described in Johnson et al. (2012). The study protocol was approved by the University of Wisconsin-Madison Health Sciences Institutional Review Board. All subjects gave written informed consent and were screened for neurological and psychiatric conditions and other risk factors related to the application of TMS before participation.

### Experimental Task and Procedure

Single pulses of TMS were delivered to the SPL during the delay period of a spatial STM task. Each trial of the task began with a 1,000-ms fixation period followed by the sequential presentation of four memory targets at different, randomly selected screen locations. Stimulus presentation was followed by a 3,750-ms delay period, during which the central fixation cross remained visible, followed by the appearance of a probe stimulus that was present for up to 2,000 ms (Figure 1A). When the probe appeared, subjects made a yes/no button press, indicating whether the location of the probe matched the location of any one of the four memory targets (50% probability). On 50% of trials (randomly interleaved), two TMS pulses were delivered at an average rate of 0.5 Hz during the delay period: the first pulse was delivered  $750 \pm 250$  ms after delay-period onset (i.e., a minimum of

500 ms after the offset of the final memory array item), followed by the second pulse  $2,000 \pm 250$  ms later. Trials with TMS will be referred to as the TMS<sub>on</sub> trials/condition, and trials without TMS will be referred to as the TMS<sub>off</sub> trials/condition. Trials were separated by a 1,000-ms intertrial interval. A total of 160 TMS pulses were delivered across 80 TMS<sub>on</sub> trials, intermixed with an equal number of TMS<sub>off</sub> trials. Full details can be found in Johnson et al. (2012).

### TMS Targeting and Stimulation

TMS was delivered with a Magstim Standard Rapid magnetic stimulator equipped with a 70-mm figure-of-eight stimulating coil (Magstim, Whitland, UK). TMS was applied to a portion of the left SPL [Brodmann's Area (BA) 7] dorsal and medial to the intraparietal sulcus and posterior to the postcentral sulcus (Fig. 1A, inset). The SPL was identified on the basis of individual anatomy from whole brain T1-weighted anatomical MRIs that were acquired with a GE MR750 3T MRI scanner for each subject before the study (176 axial slices with a resolution of 1 mm). TMS targeting was achieved using a Navigated Brain Stimulation (NBS) system (Nextstim, Helsinki, Finland) that uses infrared-based frameless stereotaxy to map the position of the coil and the subject's head within the reference space of the individual's high-resolution MRI. TMS was delivered at an intensity of 110–140 V/m (for a given subject, intensity and coil position were held constant across the task; Rosanova et al. 2009; Casali et al. 2010). Maximum stimulator output varied from 65 to 92% (M = 82%, SD = 9%). Pulses were biphasic with a pulse duration of 0.280 ms. To avoid contamination of the EEG by auditory artifacts, masking noise was played through inserted earplugs throughout the testing session, as in previous studies (Esser et al. 2006).

### EEG Recording

EEG was recorded with a 60-channel TMS-compatible amplifier (Nextstim; Helenski, Finland), which uses a sample-and-hold circuit that holds amplifier output constant from 100  $\mu$ s pre- to 2 ms poststimulus. Electrode impedance was kept  $<3$  k $\Omega$ . There was a 0.1-Hz high-pass filter built into the amplifier. A single electrode, placed on the forehead, was used as the reference and eye movements were recorded with two additional electrodes placed near the eyes. Data were sampled at 1,450 Hz with 16-bit resolution.

### Data Preprocessing

Data were processed offline using the EEGLab toolbox (Delorme and Makeig 2004) running MATLAB R2012b (Mathworks, Natick, MA). The data were downsampled to 500 Hz, band-pass filtered between 2–80 Hz, and notch filtered at 60 Hz. Movement-related artifacts were identified and removed by visual inspection and individual electrodes exhibiting excessive noise were reinterpolated using spherical spline interpolation. All data were average referenced. Independent components analysis was then used to identify and remove components reflecting residual muscle activity, eye movements, blink-related activity, and residual TMS-related artifacts. Eye movements, blinks, and muscle artifacts were detected using standard procedures as described in (Jung et al. 2000). TMS artifacts were identified and removed as described in Hamidi et al. (2010). Greater than 91% of trials (roughly 146/160 trials per subject) remained after removal of trials containing large artifacts, resulting in an average of 146 (SD = 18) TMS pulses available for analysis per subject after data processing.

### Analysis Methods

**Overview.** The goal of the study was to determine if the power or phase immediately before TMS predicted the amplitude and/or extent of propagation of the TMS-ER on a trial-by-trial basis. We ap-

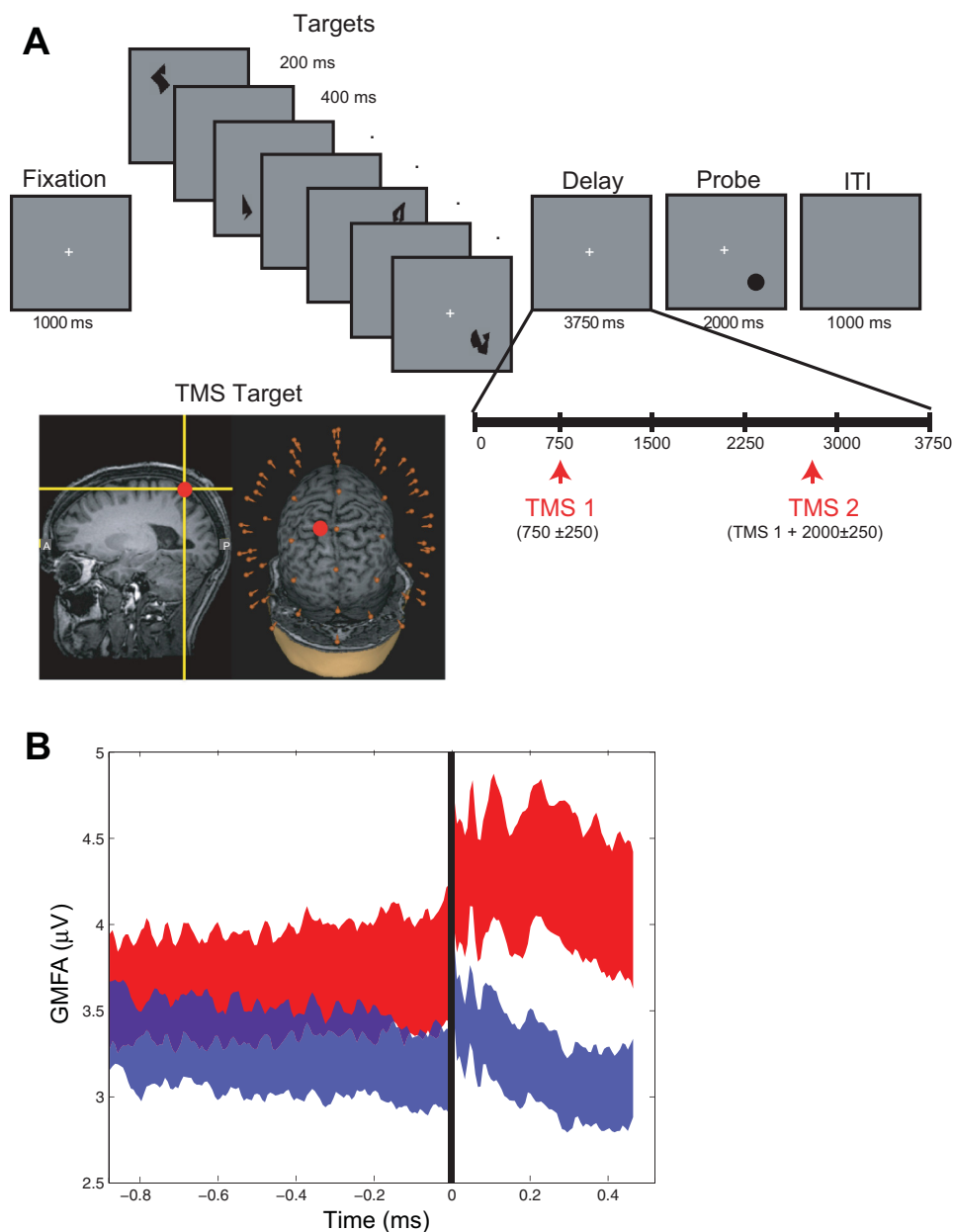


Fig. 1. *A*: short-term memory (STM) task and experimental set-up. Subjects performed a spatial STM task in which they were asked to remember the locations of the 4 shapes and indicate whether the probe's location matched a location of one of the targets. The shape of the targets is irrelevant to this task. TMS was applied to the superior parietal lobule using MRI-guide stereotaxy (*inset*). *B*: global mean field amplitude (GMFA) in High and Low bins. The GMFA averaged over subjects, sorted into High (red trace) and Low (blue trace) bins. Height and width of ribbon denotes means  $\pm$  SE. TMS delivery at *time 0* (black line). ITI, intertrial interval.

proached the problem using a two-step process. The rationale for *step 1* was that, because specific frequencies involved in determining these properties of the TMS-ER were not known a priori, we would first empirically determine candidate frequencies based on the aspects of the EEG signal that accounted for variation in the TMS-ER. Having done so, *step 2* would characterize how prestimulation phase at the frequencies identified in *step 1* influenced spectral properties of the TMS-ER measured across the scalp.

To begin *step 1*, trials were sorted by a measure of brain activation that captures the global amplitude and spread of the TMS-ER, the global mean field amplitude (GMFA; Lehmann and Skrandies 1980; Komssi et al. 2004). We then determined which frequencies showed the greatest difference in power or intertrial phase coherence (ITC; Tallon-Baudry et al. 1996) before TMS using GMFA as a dependent categorical variable. Specifically, we labeled the GMFA as being either "high" or "low" relative to the median value (Fig. 1*B*). Based on the assumption that EEG signals are derived from fluctuations in local field potentials of cortical ensembles, we assumed that oscillatory sources generating coherent signal (showing higher ITC) in particular

frequency bands would have greater collective influence on the subsequent TMS-ER than noncoherent sources (i.e., those showing relatively low ITC; Pesaran et al. 2002; Tallon-Baudry et al. 2004). Additionally, sources generating signal with high power in certain frequencies were assumed to have more "potential energy" to subsequently influence the TMS-ER than sources generating low amounts of power. It may be the case that these sources are composed of more neural elements as well. Thus relatively low power was interpreted to mean that the relative size of the underlying neural ensemble was either smaller or less activated prestimulation and thus would not have as much of an influence on the TMS-ER (quantified at the scalp level as the GMFA).

*Step 2* of the analysis was more exploratory in nature and involved characterizing how prestimulation phase at the frequencies identified in *step 1* influenced spectral properties of the TMS-ER measured across the scalp. (Note that, because prestimulation power was not found to predict the GMFA in *step 1*, power was not addressed in *step 2*.) To do so, we assessed the trial-by-trial variations in "post-TMS" power by resorting all trials now according to prestimulus phase and

the frequency and time points prestimulation, defined by *step 1* and determining the effect of phase on post-TMS power across conditions. These effects were compared with the EEG recorded during corresponding segments of a cognitively equivalent “no TMS” condition (the TMS<sub>off</sub> condition), in which participants completed the STM task in the absence of TMS. The post-TMS evoked power has been suggested to reflect resonance properties of cortico-thalamic circuits (Rosanova et al. 2009) and has been used as a measure of the “state” of the stimulated cortical networks, specifically, the state of the network “effective connectivity” (Casali et al. 2010).

**Procedures.** STEP 1. To determine which frequencies influenced the TMS-ER, we calculated the GMFA, as follows (based on Lehmann and Skrandies 1980):

$$\text{GMFA}(t) = \sqrt{\left\{ \sum_i^k [V_i(t) - V_{\text{mean}}(t)]^2 \right\} / k}$$

where  $t$  is the time point in the trial,  $i$  is the present electrode number, and  $k$  is the total number of electrodes. The GMFA was calculated from 10 to 400 ms post-TMS. We then sorted each subjects’ trials via median split into those with high or low GMFA (High and Low groups, Fig. 1B). Because TMS was delivered near channel P1, the prestimulation ITC and power were calculated for each frequency, for High and Low GMFA groups, at this channel. Both were derived from a time-frequency transformation of the data using Hanning tapers with a frequency-dependent window of three cycles/frequency analyzed, calculated from 2 to 50 Hz. Three cycles were chosen because this is the minimum number required to obtain a reliable measure of the “instantaneous phase” (Le Van Quyen et al. 2001) while still allowing estimation of phase and power in the pre-TMS interval uncontaminated by the pulse itself. (Note that this restricts the prestimulation time-window of observation to effectively 1.5 cycles per frequency of interest.) The difference between High and Low GMFA groups was compared with a surrogate distribution of difference values (power difference between High and Low GMFA groups, or ITC difference between High and Low GMFA groups) obtained through a bootstrapping procedure as follows. For each subject, trials were randomly assigned to one of two groups and a difference in power and ITC was calculated for channel P1 data. This was repeated 10,000 times per subject. From this, a grand average distribution was derived by selecting a difference sample from each subjects’ surrogate distribution and calculating a grand average difference in power or ITC. This procedure was also repeated 10,000 times. Finally, we identified clusters of frequency-time points prestimulation that showed significant differences in power or ITC (between High and Low GMFA bins) relative to this surrogate distribution, with significance differences defined as those samples showing <5% of null samples to be above the experimental sample (similar to  $P < 0.05$ ). To correct for multiple comparisons, we also identified clusters of frequency-time points that were corrected considering a false discovery rate of 5% (Benjamini and Hochberg 1995). Note that, due to the nature of EEG-derived spectrograms, however, each test is not truly independent of all the others so this correction is overly conservative, thus we present both sets of results (corrected and uncorrected).

STEP 2. Having determined that the prestimulation phase at 20 Hz and  $-150$  ms (defined by the results from *step 1*, see Fig. 2A) predicts the amplitude of the GMFA, in the second part of the analysis, we sought to characterize the relationship between prestimulation phase at this frequency and time point and the spectral properties of the TMS-ER in the beta band. We calculated the prestimulation phase of data derived from channel P1. As above, the time-frequency representation of the data was derived using Hanning tapers and a window length of three cycles, at 20 Hz and  $-150$  ms. Because the analysis was focused on discovering patterns in the data, as opposed to testing a priori predictions about the effects of stimulating at particular phase angles, the data were binned into 10 phase bins ( $36^\circ$  each). To analyze spectral properties of the TMS-ER within each bin, we calculated the

average power from 10 to 400 ms after TMS onset for each bin (using Hanning tapers, window length 3 cycles; evaluated from 15 to 25 Hz), referred to as the “TMS-evoked power.” To determine if prestimulus phase had a significant effect on the TMS-ER, we compared these data to the “null result,” the TMS<sub>off</sub> condition, which captures the naturally present relationship between ongoing phase and power fluctuations in oscillatory activity. In other words, we accounted for the relationship one might expect to exist between power and phase at one time point and the power of the signal at a subsequent time point, absent the delivery of TMS. To do this, trials from the TMS<sub>off</sub> condition were epoched into two subtrials per delay period similar to the TMS<sub>on</sub> condition, such that one set of subtrials was centered at  $750 \pm 250$  ms after delay onset and an equal number at a second time point  $2,000 \pm 250$  ms after that. For each condition, power in the 10–400 ms time window will be referred to as the “poststimulation” power, even though no TMS pulses were delivered in the TMS<sub>off</sub> condition. Similarly, the phase before *time 0* will be referred to as “prestimulation” phase. Because the pattern of effects is not known a priori, we chose to use a two-way ANOVA with phase bin (1–10) and TMS (on and off) as within subject factors to determine if prestimulation phase at a particular channel predicted poststimulation power in the beta band. Bonferroni correction (type 1 error  $\alpha = 0.05$ ) was done for multiple comparisons, although note that this test is not optimal for analysis of these data since the electrodes are contiguous in space and thus the tests are not truly independent.

## RESULTS

All subjects showed a significant difference in mean GMFA between High and Low poststimulation GMFA conditions (two-sided unpaired  $t$ -tests,  $P_s < 0.05$ ; Fig. 1B), confirming the validity of using this procedure to obtain an outcome measure for the subsequent analyses. Note there was no significant effect of TMS on performance accuracy of the spatial STM task [mean %accuracy on TMS<sub>on</sub> trials was 84.38 (SD = 8.37) and on TMS<sub>off</sub> trials was 84.06 (SD = 8.75);  $P > 0.99$ ; Johnson et al. 2012]. Furthermore, there was no effect of pulse position (*pulse 1* vs. *2*) on the categorization of GMFA (one-way ANOVA with subject as a repeated measure,  $F = 1.3$ ,  $P = 0.26$ ). We will first describe the effects of the prestimulation phase on the TMS-ER (*step 1* and *step 2* analyses), followed by consideration of the effects of prestimulation power on the TMS-ER (*step 1* only).

### TMS-ER Is Influenced by the Prestimulation Oscillatory Phase

For *step 1* of the analyses, we found that prestimulation phase in the beta and gamma bands predicted the amplitude of the TMS-ER, as measured using GMFA. Results indicated that the ITC from 15 to 25 Hz ( $-200$  to  $-150$  ms) pre-TMS, corresponding to the beta band, and from 33 to 41 Hz ( $-330$  to  $-280$  ms) and from 33 to 50 Hz ( $-180$  to  $-80$  ms) pre-TMS, corresponding to the gamma band, predicted whether the GMFA would be High or Low (all  $P_s \leq 0.05$ , uncorrected, Fig. 2A). Elevated phase coherence in these bands and time points predicted elevated GMFA from 10–400 ms post-TMS (i.e., the duration of the TMS-ER). The effect was present for each frequency within those bands (i.e., effects were present over continuous frequencies and time points). After correction for the false discovery rate, one cluster remained in the beta band (all  $P_s \leq 0.05$ , corrected, Fig. 2A).

Using this information, in *step 2* of the analysis, we determined that, for TMS<sub>on</sub> trials, poststimulation power in the beta

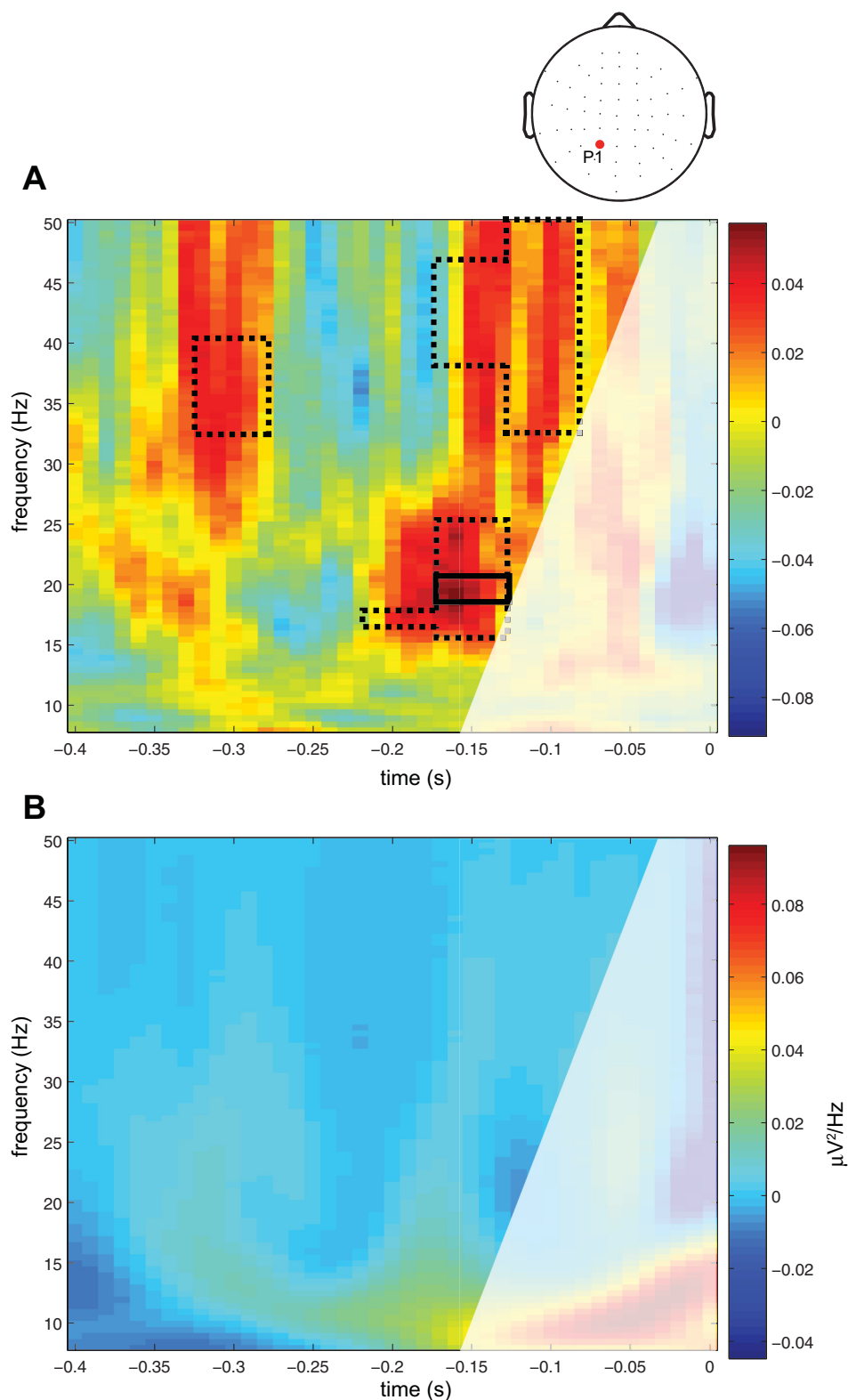


Fig. 2. Prestimulation phase or power and the GMFA. *A*: difference in intertrial phase coherence between groups of trials with either High or Low post-TMS GMFA. Clusters of time-frequency points that were significantly elevated above the null distribution shown where dashed lines delineate clusters with uncorrected *P* values, and solid lines delineate clusters with corrected *P* values. The *z*-axis showed positive differences between high and low in red/warm colors and negative differences in blue/cool colors. *B*: difference in power between High and Low GMFA trials. Same conventions as *A*. For *A* and *B*, the area delineated in white was not included in the analysis because of the possibility that it may contain contamination from the post-TMS time period due to windowing effects.

band showed maximal amplitude at particular phases at 20 Hz and at  $-150$  ms (point within the cluster that survived multiple comparisons testing, Fig. 2*A*), and these phases differed from those underlying the relationship between beta-band power and phase in the TMS<sub>off</sub> condition. We needed to account for temporal dependencies of sorting by prestimulation phase,

because it is likely that there is a relationship between phase at one time point and a later time point, regardless of the influence of TMS. To do this, we compared the TMS<sub>on</sub> condition to the cognitively equivalent TMS<sub>off</sub> condition (i.e., the TMS  $\times$  phase bin interaction; see METHODS). This analysis revealed a significant effect of prestimulation phase at 20 Hz on post-

stimulation power in the beta band in a cluster of central, parietal, and occipital electrodes that are relatively continuous in space (channels FCz, CP3, CP1, CPz, P3, P1, Pz, PO3, POz, PO4, O1, Oz, O2, and Iz; Table 1, Fig. 3A). There was a main effect of TMS at channels AF3, AFz, F1, Fz, F2, FC1, FCz, FC2, Cz, C6, TP9, CP1, CPz, CP2, TP10, P1-P8, Pz, PO3, POz, PO4, O1, Oz, O2, and Iz ( $P_s \leq 0.05$ , Table 1). There was a main effect of phase at channels AFz, AF4, Fz, F2, FC2, P3, P5, PO3, and O1 ( $P_s \leq 0.05$ , Table 1). The abovementioned channels showed a significant TMS  $\times$  phase bin interaction ( $P_s \leq 0.05$ , Table 1). On visual inspection of the data, the pattern of this effect across phase bins was qualitatively similar across these channels (Fig. 3, B and C). Poststimulation power was elevated relative to power in the TMS<sub>off</sub> condition, when the prestimulation phase in the beta band was between  $-4\pi/5$  and  $-3\pi/5$  radians ( $-143$  and  $-108^\circ$ ) and between  $\pi/5$  and  $2\pi/5$  radians ( $37$  and  $72^\circ$ ). Note the phase of the sorting frequency is shown as a “descriptive cycle” on the cumulative plot shown in Fig. 3C for illustration.

#### TMS-ER Is Not Influenced by Prestimulation Oscillatory Power

Prestimulation power did not predict the magnitude of the TMS-ER as quantified by the GMFA. Results showed no significant effects within the time windows allotted for this analysis (Fig. 2B). Because no significant clusters were found in the *step 1* analyses, *step 2* analyses were not performed for prestimulation power.

#### DISCUSSION

The present study sought to find elements of the ongoing EEG that relate to the brain's momentary state of excitability and connectivity, as measured by the TMS-ER. Specifically, we investigated whether trial-by-trial variation in prestimulation phase or power at the site of TMS predicted subsequent variations in one measure of brain activation, the TMS-ER, which is sensitive to global brain states such as sleep stages (Massimini et al. 2005), levels of clinically determined consciousness (Rosanova et al. 2012), and cognitive context (Johnson et al. 2012). The present report describes results of an analysis of data from Johnson et al. (2012) at a finer temporal scale than has previously been studied. Specifically, we investigated whether the TMS-ER was sensitive to moment-by-moment fluctuations in oscillatory activity during STM, as measured by the prestimulation phase and power across frequency bands. This question has been previously addressed during nonrapid eye movement sleep using frequencies  $<1$  Hz (Bergmann et al. 2012) but not during an awake task state.

At the whole-brain level, results obtained in *step 1* of the analysis revealed that the prestimulation phase in the beta- and gamma-frequency bands predicted the global amplitude of the TMS-ER, summarized by the GMFA. Only the beta-band cluster survived a test of multiple comparisons. In contrast, we found no reliable relationship between prestimulation power and the GMFA in any frequency band. Follow-up analysis showed that TMS-evoked power in the beta band had maximal amplitude when the prestimulation ( $-150$  ms) phase at 20 Hz was between  $-4\pi/5$  and  $-3\pi/5$  radians ( $-143$  and  $-108^\circ$ ) and between  $\pi/5$  and  $2\pi/5$  radians ( $37$  and  $72^\circ$ ). This roughly corresponds to the rising and falling slopes of a cosine curve.

Table 1. Effect of prestimulation phase at 20 Hz on poststimulation power in the beta (15–25 Hz) band across channels

Channel	Phase Bin		TMS <sub>on</sub>		Phase Bin $\times$ TMS <sub>on</sub>	
	F(9,135)	P	F(1,15)	P	F(9,135)	P
Fp1	0.890	0.536	3.453	0.083	0.724	0.686
Fpz	0.821	0.597	2.827	0.113	0.771	0.643
Fp2	0.979	0.460	0.000	0.998	0.567	0.822
AF3	1.534	0.142	4.540*	0.050	0.960	0.476
AFz	1.949*	0.050	7.268*	0.017	1.280	0.253
AF4	1.950*	0.050	3.777	0.071	0.994	0.448
F5	1.052	0.402	1.892	0.189	1.449	0.174
F3	1.313	0.235	0.012	0.914	1.147	0.335
F1	1.797	0.074	9.993*	0.006	1.419	0.186
Fz	2.325*	0.018	9.413*	0.008	1.791	0.075
F2	2.891*	0.004	4.683*	0.047	1.110	0.360
F4	1.373	0.206	0.590	0.454	1.617	0.116
F6	1.100	0.367	0.001	0.973	0.648	0.754
FT9	1.275	0.256	0.080	0.782	1.092	0.373
FT7	1.016	0.431	0.071	0.794	0.844	0.577
FC5	1.022	0.426	0.250	0.624	1.067	0.391
FC3	1.134	0.343	0.596	0.452	0.983	0.457
FC1	1.287	0.250	8.433*	0.011	0.908	0.520
FCz	1.700	0.095	9.060*	0.009	2.317*	0.019
FC2	3.314*	0.001	4.699*	0.047	0.919	0.511
FC4	1.121	0.352	0.774	0.393	0.897	0.530
FC6	0.921	0.509	1.083	0.315	0.932	0.500
FT8	1.206	0.296	0.983	0.337	1.030	0.419
FT10	1.506	0.152	0.022	0.883	1.084	0.378
T7	1.183	0.311	2.173	0.161	1.384	0.201
C5	0.840	0.580	1.311	0.270	1.030	0.420
C3	0.726	0.684	1.056	0.320	0.993	0.449
C1	0.875	0.549	3.469	0.082	1.153	0.330
Cz	1.254	0.268	15.933*	0.001	1.790	0.076
C2	0.843	0.578	2.665	0.123	1.040	0.412
C4	0.668	0.737	1.148	0.301	1.377	0.204
C6	0.809	0.609	5.044*	0.040	1.107	0.362
T8	1.161	0.325	1.869	0.192	1.367	0.209
TP9	0.917	0.512	5.144*	0.039	1.487	0.159
TP7	1.533	0.142	0.024	0.879	1.446	0.175
CP5	1.249	0.271	0.485	0.497	1.625	0.114
CP3	0.973	0.465	0.654	0.431	2.024*	0.041
CP1	1.180	0.313	10.033*	0.006	2.105*	0.033
CPz	0.903	0.524	27.176*	0.000	2.106*	0.033
CP2	0.538	0.845	4.738*	0.046	1.640	0.110
CP4	0.832	0.588	0.280	0.605	1.293	0.247
CP6	1.873	0.061	0.855	0.370	1.416	0.187
TP8	1.776	0.078	0.576	0.460	1.139	0.340
TP10	0.877	0.547	5.452*	0.034	1.137	0.341
P7	1.194	0.304	10.824*	0.005	1.575	0.129
P5	2.233*	0.023	12.186*	0.003	1.755	0.082
P3	1.961*	0.049	10.379*	0.006	2.721*	0.006
P1	1.665	0.103	7.588*	0.015	2.184*	0.027
Pz	0.465	0.896	5.817*	0.029	2.222*	0.024
P2	0.741	0.671	5.245*	0.037	1.621	0.115
P4	1.193	0.304	5.985*	0.027	1.195	0.303
P6	1.421	0.185	6.296*	0.024	1.106	0.363
P8	1.652	0.107	3.938*	0.066	1.508	0.151
PO3	2.073*	0.036	15.298*	0.001	2.067*	0.037
Poz	0.721	0.689	9.339*	0.008	2.129*	0.031
PO4	0.845	0.576	7.450*	0.016	1.953*	0.050
O1	2.811*	0.005	10.458*	0.006	2.002*	0.044
Oz	1.223	0.286	12.891*	0.003	2.499*	0.011
O2	1.164	0.323	4.321*	0.055	1.992*	0.045
Iz	1.503	0.153	16.464*	0.001	2.353*	0.017

TMS, transcranial magnetic stimulation. \* $P \leq 0.05$ .

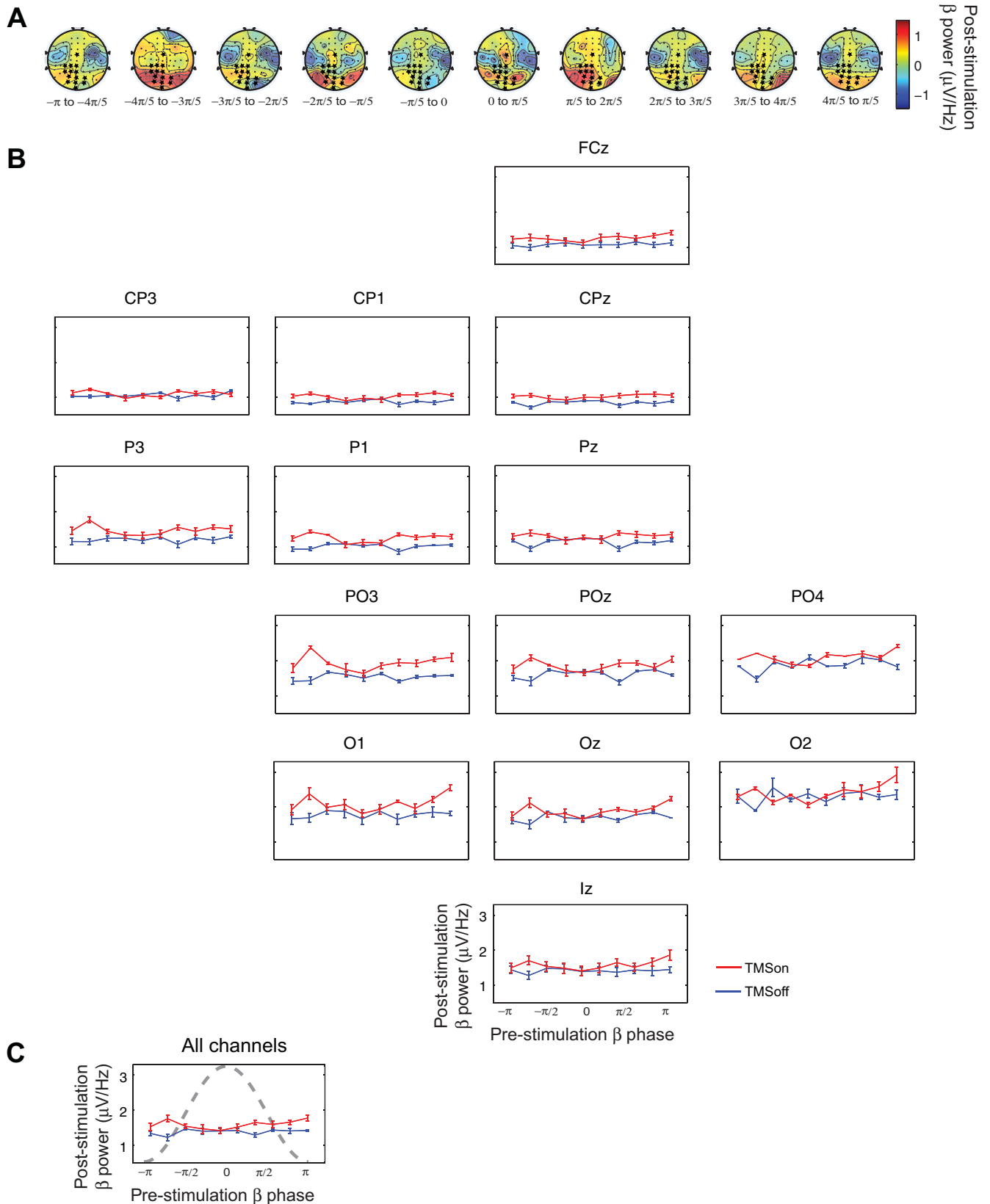


Fig. 3. Prestimulation phase at 20 Hz relates to poststimulation power in the beta band (15–25 Hz). *A*: topoplots of the difference between beta band power for TMS<sub>on</sub> minus TMS<sub>off</sub> at each phase bin. Stars mark channels that showed a significant phase bin  $\times$  TMS (TMS<sub>on</sub> vs. TMS<sub>off</sub>) interaction ( $P_s \leq 0.05$ ). *B*: beta-band power at each phase bin for channels that showed a significant phase bin  $\times$  TMS (TMS<sub>on</sub> vs. TMS<sub>off</sub>) interaction. TMS<sub>on</sub> is in red, and TMS<sub>off</sub> is in blue; 10 phase bins, from  $-\pi$  to  $\pi$ ,  $36^\circ$  per bin. Standard 10–10 electrode channel layout was used. *C*: summary: mean poststimulation beta-band power across channels shown in *B* at each phase bin with descriptive cycle of the sorting frequency in dashed gray.



To our knowledge, this observation reflects a previously undescribed means by which TMS influences ongoing brain activity. This pattern of effects was distributed across central, parietal, and occipital channels. These results provide evidence supporting the proposal that the brain's internally generated rhythms create a meaningful temporal context that determines the immediate, instantaneous brain state, as measured by the TMS-ER. Intriguingly, Monto et al. (2008) have shown that infraslow oscillations (0.0 to 0.1 Hz) organize all other spectral frequencies, which reach their peaks at  $-\pi/2$  radians of the infraslow oscillations. This property is also reflected in behavioral performance peaks. Such infraslow oscillations, it is suggested, might influence the general excitability of cortical networks. Somewhat relatedly, it has been shown in rats that long-term potentiation can be induced when high-frequency bursts are applied at the poststimulation peaks of the stimulus-induced phase reset theta wave but not at the troughs (Hölscher et al. 1997). Although at present this is little more than speculation, these effects might account for why, in the present study, the TMS-ER was largest at the rising and falling phase-to-peak of the sorting (beta band) frequency. It is important to keep in mind, however, that the observations made in the *step 2* analysis are preliminary and require follow-up in a properly designed experiment with greater numbers of trials. In general, the origin of high-frequency oscillations, such as the beta and gamma bands, is not known, and furthermore, it is not known how polarity shifts might change with recording electrode and reference position.

The sensitivity of the TMS-ER to prestimulation phase is in line with the general theory that underlying oscillations produce fluctuations in cortical excitability (Bishop 1933; Buzsáki and Draguhn 2004). A related possibility, particularly relevant for our *step 2* analysis, is that these results reflect increased communication between distal brain regions, without involving an increase in excitability per se. For example, it is possible that a distal region could be at an equivalent level of excitability on two trials, but if the inputs are more effectively phase synchronized on *trial B* than on *trial A*, that the evoked response to *trial B* would be greater. These two possibilities are by no means mutually exclusive. By either explanation, our data support the proposal that fluctuation in the phase of an underlying oscillation effectively creates "windows of excitability" during which the brain, or a particular brain area, is in a state that is more open to perturbation or communication with other brain areas (Dugué et al. 2011). We find that this is literally true in the context of TMS. The TMS-evoked power in the beta band is larger when TMS is delivered at particular phases of that band. In the context of a subject performing a STM task, the prestimulation phase in the beta band predicted subsequent effects in the poststimulation beta-band power.

Interestingly, we did not find a significant relationship between prestimulation power and GMFA. Although either of these findings may seem to be at odds with some of the literature reviewed in the introduction, there are important methodological differences to keep in mind. One feature of the present study was the restricted time window during which we could assess prestimulation effects: from 500 ms prestimulation to 1.5 cycles (per frequency) prestimulation. Thus we cannot rule out the possibility that effects of prestimulus power might be present in our data if power could have been estimated at time points closer to TMS delivery. As for compar-

ison to studies using visual perception as the dependent measure, it may be that fluctuations in alpha-band power that predict such factors as phosphene and stimulus detection thresholds reflect relatively local dynamics within the occipital cortex, whereas the power fluctuations observed during a visual STM task, such as that featured in the present study, likely reflect long-range interactions between distal brain areas, including frontoparietal regions (Kundu et al. 2013). If this were the case, regional phase synchronizing long-range connectivity would be more pronounced in the case of complex tasks such as STM compared with relatively regional phenomena such as visual perception.

In general, the results from the present study provide empirical support for theoretical accounts that fluctuating phase of ongoing oscillations creates windows of excitability in the brain. Furthermore, they give insight into how TMS interacts with ongoing brain activity on a pulse-by-pulse basis. Thus they are applicable to understanding the electrophysiological and biological underpinnings of studies using single-pulse as well as repetitive TMS for a wide range of applications from basic science to medicine.

#### ACKNOWLEDGMENTS

We thank Dr. Olivia Gosseries for thoughtful comments regarding the manuscript.

#### GRANTS

This study was supported by National Institute of Mental Health Grants MH-095428 (to B. Kundu), MH-88115 (to J. S. Johnson), and MH-064498 and MH-095984 (to B. R. Postle).

#### DISCLOSURES

No conflicts of interest, financial or otherwise, are declared by the author(s).

#### AUTHOR CONTRIBUTIONS

Author contributions: B.K., J.S.J., and B.R.P. conception and design of research; B.K. and J.S.J. performed experiments; B.K. analyzed data; B.K., J.S.J., and B.R.P. interpreted results of experiments; B.K. prepared figures; B.K. drafted manuscript; B.K., J.S.J., and B.R.P. edited and revised manuscript; B.K., J.S.J., and B.R.P. approved final version of manuscript.

#### REFERENCES

- Babiloni C, Vecchio F, Bultrini A, Luca Romani G, Rossini PM.** Pre- and poststimulus alpha rhythms are related to conscious visual perception: a high-resolution EEG study. *Cereb Cortex* 16: 1690–700, 2006.
- Benjamini Y, Hochberg Y.** Controlling the false discovery rate: a practice and powerful approach to multiple testing. *J R Stat Soc Ser B* 57: 289–300, 1995.
- Bergmann TO, Mölle M, Schmidt M, Lindner C, Marshall L, Born J, Siebner HR.** EEG-guided transcranial magnetic stimulation reveals rapid shifts in motor cortical excitability during the human sleep slow oscillation. *J Neurosci* 32: 243–253, 2012.
- Bishop GH.** Cyclic changes in excitability of the optic pathway of the rabbit. *Am J Psychiatry* 103: 213–224, 1933.
- Busch NA, Dubois J, VanRullen R.** The phase of ongoing oscillations predicts visual perception. *J Neurosci* 31: 11889–11893, 2011.
- Busch NA, VanRullen R.** Spontaneous EEG oscillations reveal periodic sampling of visual attention. *Proc Natl Acad Sci USA* 107: 16048–16053, 2010.
- Bushman TJ, Miller EK.** Serial, covert shifts of attention during visual search are reflected by the frontal eye fields and correlated with population oscillations. *Neuron* 63: 386–396, 2009.
- Buzsáki G, Draguhn A.** Neuronal oscillations in cortical networks. *Science* 304: 1926–1929, 2004.

- Casali AG, Casarotto S, Rosanova M, Mariotti M, Massimini M. General indices to characterize the electrical response of the cerebral cortex to TMS. *Neuroimage* 49: 1459–1468, 2010.
- Delorme A, Makeig S. EEGLAB: an open source toolbox for analysis of single-trial EEG dynamics including independent component analysis. *J Neurosci Methods* 134: 9–21, 2004.
- Van Dijk H, Schoffelen JM, Oostenveld R, Jensen O. Prestimulus oscillatory activity in the alpha band predicts visual discrimination ability. *J Neurosci* 28: 1816–1823, 2008.
- Dugué L, Marque P, VanRullen R. The phase of ongoing oscillations mediates the causal relation between brain excitation and visual perception. *J Neurosci* 31: 11889–11893, 2011.
- Engel AK, Fries P. Beta band oscillations—signalling the status quo. *Curr Opin Neurobiol* 20: 156–165, 2010.
- Esser SK, Huber R, Massimini MJ, Peterson MJ, Ferrarelli F, Tononi G. A direct demonstration of cortical LTP in humans: a combined TMS/EEG study. *Brain Res Bull* 69: 86–94, 2006.
- Hamidi M, Slagter HA, Tononi G, Postle BR. Brain responses evoked by high-frequency repetitive transcranial magnetic stimulation: an event-related potential study. *Brain Stimul* 3: 2–14, 2010.
- Hölscher C, Anwyl R, Rowan MJ. Stimulation on the positive phase of hippocampal theta rhythm induces long-term potentiation that can be depotentiated by stimulation on the negative phase in area Ca1 in vivo christian ho. *J Neurosci* 17: 6470–6477, 1997.
- Jensen O, Mazaheri A. Shaping functional architecture by oscillatory alpha activity: gating by inhibition. *Front Hum Neurosci* 4: 186, 2010.
- Johnson JS, Kundu B, Casali AG, Postle BR. Task-dependent changes in cortical excitability and effective connectivity: a combined TMS-EEG study. *J Neurophysiol* 107: 2383–2392, 2012.
- Jung TP, Makeig S, Humphries C, Lee TW, McKeown MJ, Iragui V, Sejnowski TJ. Removing electroencephalographic artifacts by blind source separation. *Psychophysiology* 37: 163–178, 2000.
- Komssi S, Kähkönen S, Ilmoniemi RJ. The effect of stimulus intensity on brain responses evoked by transcranial magnetic stimulation. *Hum Brain Mapp* 21: 1541–1564, 2004.
- Kundu B, Sutterer DW, Emrich SM, Postle BR. Strengthened effective connectivity underlies transfer of working memory training to tests of short-term memory and attention. *J Neurosci* 33: 8705–8715, 2013.
- Lange J, Oostenveld R, Fries P. Reduced occipital alpha power indexes enhanced excitability rather than improved visual perception. *J Neurosci* 33: 3212–3220, 2013.
- Le Van Quyen M, Foucher J, Lachaux J, Rodriguez E, Lutz A, Martinerie J, Varela FJ. Comparison of Hilbert transform and wavelet methods for the analysis of neuronal synchrony. *J Neurosci Meth* 111: 83–98, 2001.
- Lehmann D, Skrandies W. Reference-free identification of components of checkerboard-evoked multichannel potential fields. *Electroencephalogr Clin Neurophysiol* 48: 609–621, 1980.
- Massimini M, Ferrarelli F, Huber R, Esser SK, Singh H, Tononi G. Breakdown of cortical effective connectivity during sleep. *Science* 309: 2228–2232, 2005.
- Mathewson KE, Gratton G, Fabiani M, Beck DM, Ro T. To see or not to see: prestimulus alpha phase predicts visual awareness. *J Neurosci* 29: 2725–2732, 2009.
- Monto S, Palva S, Voipio J, Palva JM. Very slow EEG fluctuations predict the dynamics of stimulus detection and oscillation amplitudes in humans. *J Neurosci* 28: 8268–8272, 2008.
- Palva S, Palva JM. Functional roles of alpha-band phase synchronization in local and large-scale cortical networks. *Front Psychol* 2: 204, 2011.
- Pesaran B, Pezaris JS, Sahani M, Mitra PP, Andersen AR. Temporal structure in neuronal activity during working memory in macaque parietal cortex. *Nat Neurosci* 5: 805–811, 2002.
- Romei V, Brodbeck V, Michel C, Amedi A, Pascual-Leone A, Thut G. Spontaneous fluctuations in posterior alpha-band EEG activity reflect variability in excitability of human visual areas. *Cereb Cortex* 18: 2010–2018, 2008.
- Rosanova M, Casali A, Bellina V, Resta F, Mariotti M, Massimini M. Natural frequencies of human corticothalamic circuits. *J Neurosci* 29: 7679–7685, 2009.
- Rosanova M, Gosseries O, Casarotto S, Boly M, Casali AG, Bruno MA, Mariotti M, Boveroux P, Tononi G, Laureys S, Massimini M. Recovery of cortical effective connectivity and recovery of consciousness in vegetative patients. *Brain* 135: 1308–1320, 2012.
- Scheeringa R, Petersson KM, Oostenveld R, Norris DG, Hagoort P, Bastiaansen MC. Trial-by-trial coupling between EEG and BOLD identifies networks related to alpha and theta EEG power increases during working memory maintenance. *Neuroimage* 44: 1224–1238, 2009.
- Schroeder CE, Lakatos P. Low-frequency neuronal oscillations as instruments of sensory selection. *Trends Neurosci* 32: 9–18, 2009.
- Tallon-Baudry C, Bertrand O, Delpuech C, Pernier J. Stimulus specificity of phase-locked and non-phase-locked 40 Hz visual responses in human. *J Neurosci* 16: 4240–4249, 1996.
- Tallon-Baudry C, Mandon S, Freiwald AW, Kreiter AK. Oscillatory synchrony in the monkey temporal lobe correlates with performance in a visual short-term memory task. *Cereb Cortex* 14: 713–720, 2004.
- Walsh V, Pascual-Leone A. *Transcranial Magnetic Stimulation: A Neurochronometrics of Mind (Bradford Books)*. Cambridge, MA: MIT Press, 2003.
- Wyart V, Tallon-Baudry C. How ongoing fluctuations in human visual cortex predict perceptual awareness: baseline shift versus decision bias. *J Neurosci* 29: 8715–8725, 2009.